



THE INFLUENCE OF IRRADIATION ON CARBON NANOTUBES

Scutaru M.L.¹, Chircan E.¹, Limbasan M.M.¹, Oancea I.¹

¹ Transilvania University, Brasov, ROMANIA, lscutaru@unitbv.ro, chircan.eliza@unitbv.ro, m.limbasan@gmail.com, iuliana.oancea@student.unitbv.ro

Abstract: The main objective of the paper is the realization of hybrid nano-composites such as polymer-nanostructured reinforcing agent. The central idea of the paper is that by using nano-scale reinforcements, both alone and in complementarity with micro-structures, the final products will have superior properties and characteristic performance after irradiation.

Keywords: irradiation, materilas, nanotubes

1. INTRODUCTION

Compared to traditional composite materials, nano-composite materials have advantages such as structure homogeneity, improving or maintaining processability, do not have fiber breaks and in most cases, remain optically clear. Much effort has been devoted to the incorporation of nanoparticles into polymeric matrices, but few researchers have attempted to use nano-reinforcements in traditional composite structures. This technology could greatly increase the performance of these composite materials.

Polymer-based nano-composites are a class of hybrid materials composed of a polymeric matrix and an inorganic filler that has at least one of the dimensions in the nano-metric range (<100 nm) [1].

The advantages of nano-structured particles over micro ones in polymer matrices were reported almost 20 years ago [5] but the practical application was realized only after 1990, mainly due to the pioneering efforts of Toyota Motor Co. which led to the nylon-6 / clay hybrid and which became the first practical example of the use of polymeric nano-composites in the automotive industry [6].

There are two possible structures with high symmetry for nanotubes, namely: "zigzag" and "armchair" (figure 1). It is practically believed that most nanotubes do not have this high symmetry but have a "chiral" structure in which the hexagons are arranged helically around the axis of the tube. There is a close connection between the structure and properties of carbon nanotubes.

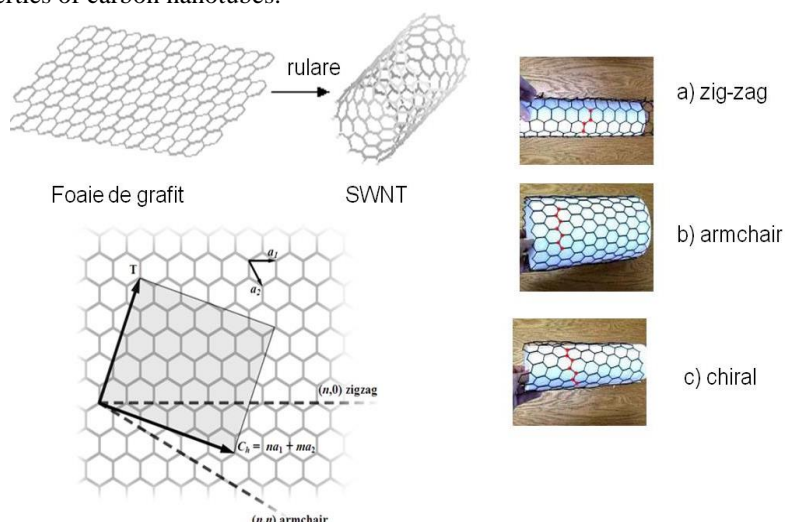


Figure 1: Different chiral vectors and chiral angles θ . Nanotube armchair, zigzag tube and chiral tube

Some of the first experimental studies on a variety of carbon materials, including unpurified nanotube samples at zero to room temperature, showed that nanotube samples at zero to room temperature showed a different behavior from the others, having a wide diamagnetic susceptibility that increases with decreasing temperature [82]. The results clearly indicated that the nanotubes have a higher susceptibility than graphite, without being

able to give an indication, when the tubes are rotated, where the susceptibility is parallel or perpendicular to the axis of the tube. It has been speculated that this wide susceptibility may be due to circular currents around the circumference of the tubes.

2. THE INFLUENCE OF IRRADIATION

To investigate the structure of atoms, the most efficient method is the one by which the matter is bombarded with high-velocity animated particles - electrons, α particles - that can thus penetrate inside atoms. From the changes of the motion of these particles, when passing through matter, conclusions can be drawn regarding the structure of atoms.

The optical spectra of atoms and X-rays provide valuable data about the structure of atoms and the phenomena that takes place inside them.

Condensed bodies emit radiation whose spectrum is continuous.

Incandescent gaseous substances can emit radiation whose spectrum is discrete, containing only certain wavelengths. Atomic emission spectra are obtained by detecting radiation emitted by a convenient source using a spectral apparatus (spectroscope or spectrograph). The radiation enters the device through a narrow linear slit, and the resulting atomic spectrum is presented as a succession of linear images of the slit, each radiation of a certain wavelength in the incident radiation corresponding to a spectral line. The spectrum obtained is called the line spectrum.

It has been experimentally established that atoms of incandescent gases emit spectra of lines and that these lines form well-defined groups, called spectral series.

3. MATERIAL AND WORK METHOD

After the discovery of artificial radioactivity and the construction of nuclear radiation generating installations, this problem arose even more acutely given the expansion of research and practical applications of this radiation. In addition, the fact that the presence of nuclear radiation cannot be perceived directly by man through the senses has required, for protection reasons, the design and use of devices capable of recording the presence and measuring the parameters of that radiation.

At the base of the laser pyrolysis process is the phenomenon of resonant absorption of IR radiation of a certain wavelength. Absorption is an attribute of the phenomenon of radiation selectivity (primary selectivity) that occurs at the temperature of the gaseous medium T_0 characteristic of the translation-rotation energy of the unexcited molecule.

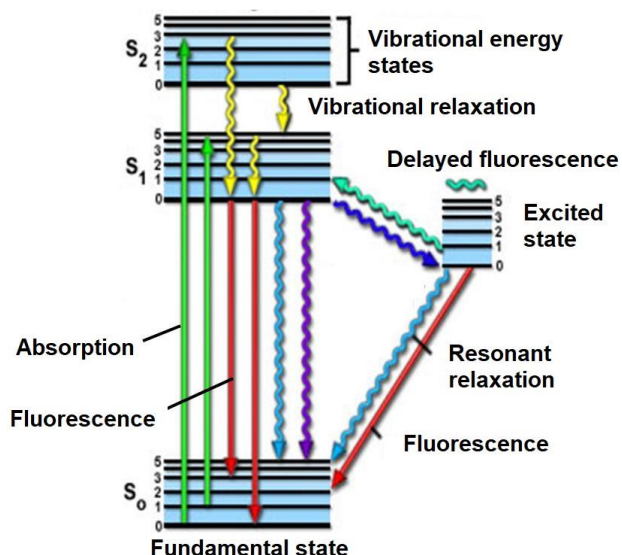


Figure 2: Jablonski energy diagram, illustrating resonant (straight line) and non-resonant (broken line) processes, applicable to the excitation mechanism of precursors

In the process of synthesis of carbon nanostructures by laser pyrolysis of gaseous or vapor hydrocarbons, the reaction is initiated as a result of the interaction between the laser beam and at least one of the reactant gases. The selection of the reaction compounds is made according to the characteristics of the process and the final product pursued. They must be in a gaseous state, at ordinary temperature (for example: acetylene) or liquids

with an acceptable vapor pressure (such as benzene), have a high carbon content / moll and last but not least absorb the incident laser radiation. The physic-chemical characteristics of such precursors (hydrocarbons) are presented in table 1.

In case of absorption of laser radiation (resonant process) at the wavelength $\lambda = 10.6\mu\text{m}$ (944cm^{-1}) the precursors decompose absorbing this radiation:



Table 1: Physic-chemical characteristics of some hydrocarbons

Precursor	Molecular mass	%C	%H	Melting temperature (°C)	Boiling temperature (°C)	Density (g/cm ³)	Absorption at $\lambda=10,6\mu\text{m}$ (cm ⁻¹)
Acetylene C ₂ H ₂	26	92,3	7,7	-81,8	Sub.	0,6181 (-82°C)	-
Ethylene C ₂ H ₄	28	85,7	14,3	-169,15	-104	0,00126 (0°C)	949,3
1,3butadiena C ₄ H ₆	54	88,9	11,1	-108,9	-4,4	-	907,8 989,7
Benzene C ₆ H ₆	78	92,3	7,7	5,5	80,1	0,8787 (15°C)	-

Ethylene (85.7% C / moll) can play both the role of carbon donor and sensitizer because it absorbs ($\nu_7 = 949\text{cm}^{-1}$) laser radiation (944cm^{-1}) and has a flame ignition threshold and energy dissociation rate (D0 [C₂H₃-H] = 4.4eV; D0 [H₂C-CH₂] = 7.9eV) quite low. Its relatively sufficient absorption of laser radiation, as well as its low dissociation energy makes this simple hydrocarbon an acceptable sensitizer for use in the case of unreasonable pyrolysis processes. At the same time, having a fairly high carbon / moll content, it can also be used successfully as a carbon donor.

The main fundamental modes of vibration of the acetylene molecule: are far ($\nu_1 = 3374\text{cm}^{-1}$, $\nu_2 = 1974\text{cm}^{-1}$, $\nu_3 = 3287\text{cm}^{-1}$, $\nu_4 = 612\text{cm}^{-1}$, $\nu_5 = 729\text{cm}^{-1}$) from the laser emission line with continuous wave of CO₂ from $10.6\mu\text{m}$ (944cm^{-1}) and for this it is necessary to introduce the sensitizer.

Known sensitizers that show absorption for CO₂ laser radiation on ethylene wool and sulfur hexafluoride include silane and boron tri-chloride whose physicochemical properties are shown in Table 2.

Due to the high temperatures in the hydrocarbon pyrolysis flame, the reactants are expected to dissociate as a result of the transfer of collisional energy from the vibrational excited molecules of the sensitizer.

Table 2: Physic-chemical properties of some sensitizers with absorption at $\lambda = 10.6\mu\text{m}$

Sensitizer	Molecular mass	Melting temperature (°C)	Boiling temperature (°C)	Density (g/cm ³)	Absorption at $\lambda=10,6\mu\text{m}$ (cm ⁻¹)
SF₆	146	-50,5	63,8	0,0066	947,5
SiH₄	32	-185	-111,8	0,0014	974,6
BCl₃	117	-107,3	12,5	1,349	956
C₂H₄	28	-169,15	-104	0,00126	949,3
Fe(CO)₅	195,90	-20	103	1,45	

The reaction is initiated as a result of the interaction between the laser beam and the reactant gases (figure 3). The system is based on a cross-shaped configuration, where the beam of a CO₂ laser (focused or not) intersects the precursor gases orthogonally. This interaction is materialized by a bright, smoky flame. Pyrolysis of the reactive gases takes place in a small vessel, well defined by the intersection of the laser-flux reactive gas beam. The nucleated particles are entrained by the gas stream and collected outside the reactor.

IR photons are absorbed by the reactant gas; the absorbed photon energy is converted into thermal energy which causes an increase in the number of collisions between the reactant gas molecules and lead to an energy transfer followed by the decomposition of the reactant gas and the formation of the base solid.

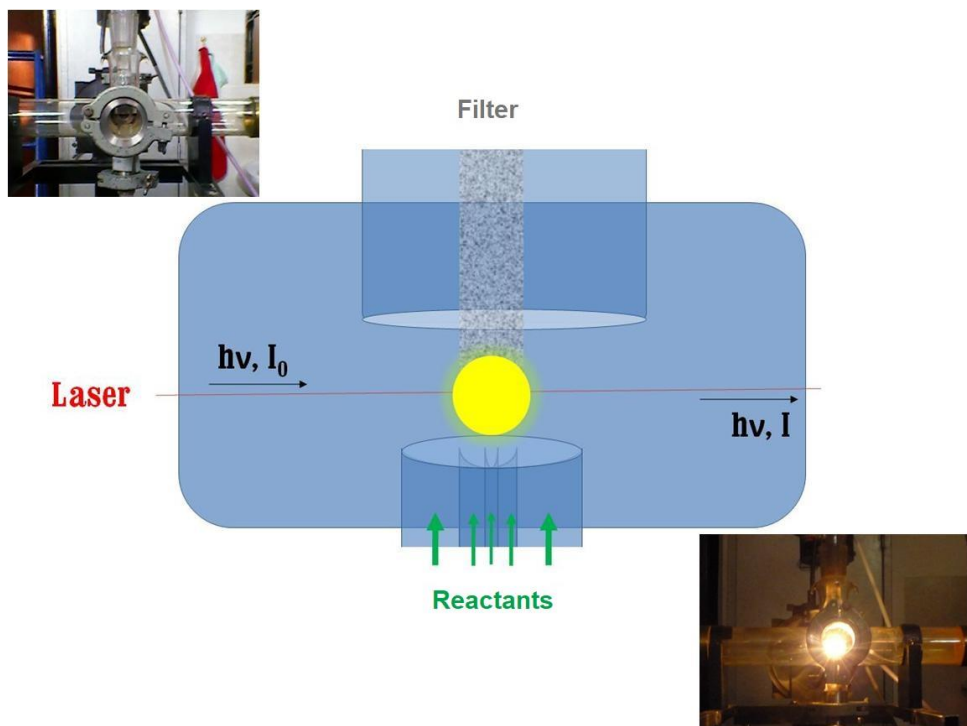


Figure 3: Principle of the laser pyrolysis synthesis method

Continuously operating CO₂ laser radiation (maximum power of 100W) passes orthogonally through the gas streams that have been introduced into the reaction chamber through three concentric nozzles. Fe (CO) 5 vapors, driven by a stream of ethylene, were introduced through the central tube while a mixture of hydrocarbons (including C₂H₂ and C₂H₄) passed through the middle tube. These reactive gas streams were confined to the flow axis by a coaxial argon stream. Ethylene (C₂H₄) was used as a sensitizer. The nucleated particles are entrained by the gas flow to a collection chamber provided with a micro-porous filter in the direction of the rotary pump. The experimental parameters used to obtain Fe / C nano-powders are presented in the following table:

Table 3: Experimental data for CF samples

Sample	Ethylene at Fe(CO) ₅	C ₂ H ₄ in	T(°C) flame	C ₂ H ₂ /Ar in	Ar confinement	Ar windows	P laser	Pressure (mbar)	M (g)
CF1	10	0	1350	130	2500	150	87/72	500	1.65
CF2	10	0	1537	130	2500	150	87/72	700	1.8
CF3	10	0	1585	130	2500	150	87/72	900	2.61

Carbon powder results from an incomplete combustion process or the thermal decomposition of hydrocarbons. Together they also form a significant number of other organic compounds. The incomplete combustion process involves the removal of hydrogen from the reaction medium and the conversion of the entire amount of carbon consumed into a useful product.

The size of the nanoparticles can be estimated by investigation with an electron microscope.

The high resolution images of electronic microscopy obtained show us a spheroidal geometry of the nano-metric carbon particles obtained by the laser pyrolysis method (figure 4) having a varied structure, but close to that of OLCs.

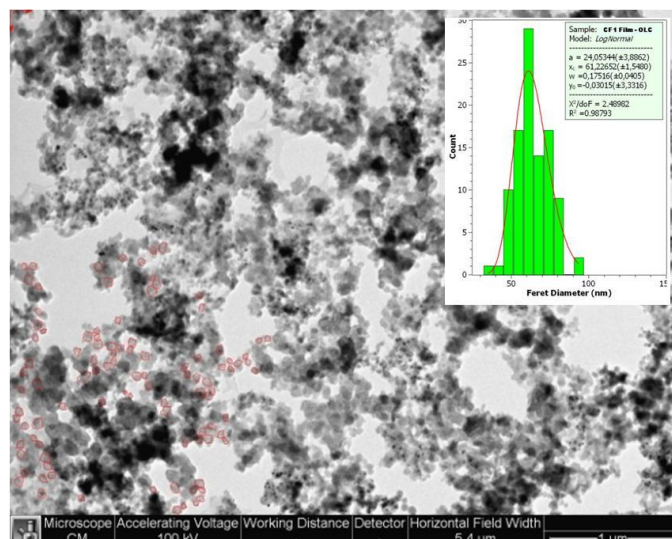


Figure 4: Distribution of OLCs in sample CF1

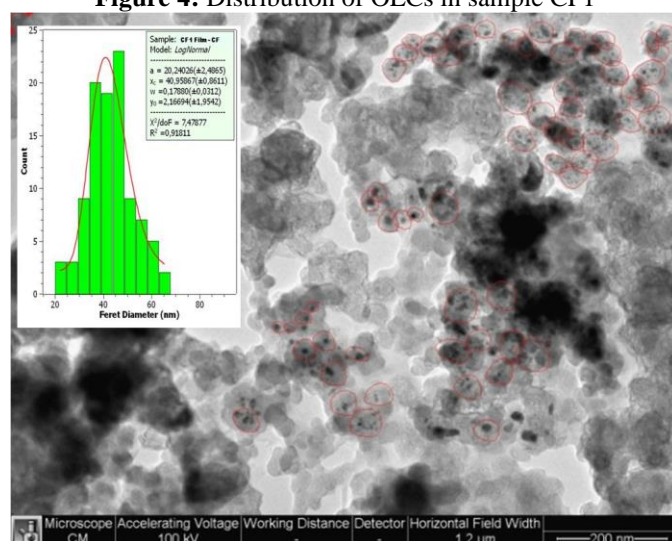


Figure 5: Distribution of carbon with encapsulated iron in sample CF1

3. CONCLUSION

Due to the fact that nano-metric carbon particles are obtained in powder form, an absolute density of the obtained powders cannot be defined and implicitly measured. Nano-metric carbon particles are defined by a specific surface area (hundreds of m^2/g) for those obtained in the laboratory, with an order of magnitude larger than micrometric carbon powders; the large specific surface area gives them a high degree of chemical reactivity, the role of catalyst of nano-metric carbon particles in hydrogenation / dehydrogenation reactions being known in the literature [23].

Characteristics of laser pyrolysis give the obtained nano-metric powder the following qualities: small dimensionality (nano-metric) and large specific surface area of particles, high degree of dimensional mono-dispersion of particles, morphology and controlled structure of particles, high purity of the obtained powders.

Electron microscopy analysis of films obtained from nano-carbon powders led to the observation of OLC structures with values from 61.22 nm for CF1 powder, 43nm for CF2 powder and 25.57nm for CF3 powder. The iron particles (10.23nm - CF1, 13.59 - CF2 and 9.45nm - CF3) are encapsulated in carbon layers, the particle size being for each investigated sample of 40.96nm - CF1, 60nm - CF2 and 32 respectively, 03nm - CF3.

REFERENCES

- [1] Stein S E, Fahr A, J. Phys. Chem. 89 (19 Milliken J, Keller T M, Baronavski A P, McElvany S V, Callahan J H, Nelson H H, Chem. Materials 3, (1991) 386
- [2] Saxby J, Chatfield P E, Vassallo A M, Wilson M A, Pang L S K, J. Phys. Chem 196 (1992) 17

- [3] Schulman J M, Disch R L, J. Chem. Soc. Chem. Commun. (1991) 411
- [4] Richter H, Fonseca A, Emberson S C, Gilles J M, Nagy J B, Thiry P A, Caudano R, Lucas A A, J. Chim. Phys. 92 (1995) 1272
- [5] Tenegal F, Petcu S, Herlin-Boime N, Armand X, Mayne M and Reynaud C, Chem. Phys. Lett. 335 (2001) 155
- [6] Ténégal F, Voicu I, Armand X, Herlin-Boime N, Reynaud C, Chem. Phys. Lett. 379, 1-2 (2003) 40-46
- [7] Alexandrescu R, Armand X, Cauchetier M, Herlin N, Petcu S and Voicu I, Carbon 36 (1998) 1285... nanoranforsări în structurile compozite tradiționale
- [8] Pinnavaia TJ, Beall GW, Eds., In „Polymer Clay Nanocomposites”. Wiley, New York 200
- [9] Clegg DW, Collyer AA, in „Mechanical Properties of Reinforced Thermoplastics”, Elsevier 1986
- [10] Choi J, Harcup J, Yee AF, Zhu Q, Laine RM, J. Am. Chem. Soc., 2001; 123; 11420 [11]. Mark JE, Lee CY-C, Bianconi PA, Eds., „Hybrid Organic-Inorganic Composites”, Vol. 585, American Chemical Society, Washington DC 1995
- [12] Sumita M, Shizuma T, Misasaka K, Ishikawa K, J. Macromol. Science .1983, B22, 601 [13]. Karauchi T, Okada A, Nomura T, Nishio T, Saegusa S, Deguchi R, SAE Tech. Pap. Ser. 1991, 910, 584
- [14] Aharoni SM, „n-Nylons: Their Synthesis, Structure and Properties”, John Wiley and Sons, Chichester 1997
- [15] Nielsen LE, Landel RF, in „Mechanical Properties of Polymers and Composites”, Marcel Dekker, New York 1994
- [16] Dresselhaus M S, Dresselhaus G, Eklund P C, Science of fullerenes and carbon nanotubes (Academic Press, New York, NY, San Diego, CA, 1996)
- [17] Iqbal Z., Structure, properties and applications of nanostructured carbon architectures, in Nanostructured Carbon for Advanced Applications, G. Benedek et al eds.), 2001 Kluwer Academic Publishers, p. 309
- [18]. Paul Holister; J. W. Welter; Cristina Romanov; Tin Harper: Introduction to nanoparticles – Cientifica 2003
- [19] Harris SJ, Weiner AM. Chemical kinetics of soot particle growth. Annu Rev Phys Chem 1985;36:31-52
- [20] London, F. Superfluids , Wiley, New York, 1950
- [21] Niels Bruckner , Richard Packard, Large area multiturn superfluid phase slip gyroscope, Journal of Applied Physics 93, 1798 (2003)
- [22] A. Lenef, T.D. Hammond, E.T. Smith, M.S. Chapman, R.A. Rubenstein and D.E. Pritchard, Phys. Rev. Lett. 78, 760 (1997) [23]. J.F. Clauser, Physica B, 151, 262 (1988).
- [24] K. Schwab, N. Bruckenr, R.E. Packard, Nature (London) 386, 585 (1997).